0630

Joint optimization of multi-echo reconstruction and quantitative map estimation in Looping Star

Haowei Xiang[1], Ilhan Kemal Onder[2], Anahita H Mehta[2], Jeffrey A Fessler[1], and Douglas C Noll[3]
[1]Electrical Engineering and Computer Science, University of Michigan, Ann Arbor, MI, United States, [2]Department of Otolaryngology-Head and Neck Surgery, University of Michigan, Ann Arbor, MI, United States, [3]Biomedical Engineering, University of Michigan, Ann Arbor, MI, United States

Synopsis

Keywords: Image Reconstruction, Quantitative Imaging, Reconstruction

Motivation: Looping-star sequences, despite their advantages, exhibit low SNR and undersampling artifacts compared to standard GRE sequences.

Goal(s): This work proposes to jointly reconstruct multi-echo data and estimate quantitative maps in looping-star to boost the SNR, reduce the undersampling artifacts, and improve image quality.

Approach: Our approach frames echo image reconstruction and quantitative map estimation as a unified optimization problem. This is then split into two sub-problems, addressed alternately using CG-SENSE.

Results: Compared to individual echo reconstruction, our joint optimization improves tSNR of both echo images and T2* maps and effectively mitigates image artifacts.

Impact: Our method jointly reconstructs multi-echo data in looping-star, enhancing SNR and reducing artifacts, with a notable tSNR improvement. It can be adapted to the Looping-Star fMRI protocol to potentially improve functional activity estimation.

Introduction

Functional magnetic resonance imaging (fMRI) is crucial for the noninvasive imaging of human brain activity, yet the intrusive acoustic noise of MRI poses challenges. This noise can induce discomfort and anxiety, especially in children or dementia patients, and can also confound sensory stimuli, affecting the BOLD response based on its loudness and duration [1].
Looping-Star, a silent MRI pulse sequence, is beneficial for pediatric MRI and auditory fMRI tasks but is hampered by sparse radial sampling and low SNR, restricting its spatial and temporal resolution [2]. We introduce a multi-echo signal collection method in the fMRI protocol to enhance sampling efficiency and SNR. We present a novel joint optimization approach for multi-echo image reconstruction and quantitative map estimation, subsequently divided into two sub-problems, which are solved by alternating minimization. After all frames are reconstructed, we use UNFOLD [3] to double the temporal resolution and reduce undersampling artifacts.

Methods

Pulse sequence: Figure 1 shows the pulse sequence we used for experiments. We optimized some parameters to improve the robustness and performance of the pulse sequence. We used a 3D generalized golden-angle-based rotation [4], reduced the number of RF pulses to 23 with increased sampling time, and increased the volume TR to 3.2 sec to reduce the undersampling artifact. Lastly, we collect 2 GRE echoes with TE = 30 and 56.9 msec respectively to improve the SNR. The sampling pattern alternates every volume TR to enable UNFOLD [5] filtering after reconstruction.
Problem formulation: In Looping-Star MRI, gradient echoes are overlapped in the time domain due to multiple RF pulses. Previous looping-star methods for fMRI typically reconstruct T2*-weighted images from a single set of GRE echoes. In contrast, in this work we use two sets of GRE echoes and then jointly reconstruct the first echo image ϱ and the exponential rate map z from the k-space data using the following optimization formulation:

$$\hat{\varrho}, \hat{z} = \arg\min_{\varrho, z} \left\| \begin{pmatrix} s_f \\ s_g \end{pmatrix} - \begin{pmatrix} A_f & 0 \\ 0 & A_g \end{pmatrix} \begin{pmatrix} \varrho \\ \varrho \odot z \end{pmatrix} \right\|_2^2 + \beta_1 R_1(\varrho) + \beta_2 R_2(z),$$

where s_f and s_g are signals from 1st and 2nd echoes respectively, A_f and A_g account for overlapping echoes as described in [6] for 1st and 2nd echoes respectively, $\odot$ is element-wise product, $R_1(\varrho)$ and $R_2(z)$ are regularizers for the echo images and rate maps. The total cost function is then divided into two sub-problems and we use an alternating approach to update ϱ and z. The ϱ and z used our prior model-based reconstruction for overlapping echoes, aiming for superior temporal resolution.
Reconstruction: We used CG-SENSE and spatial 3D quadratic roughness regularizers for both ϱ and z update. We used 20 outer iterations to alternate between updates for z and ϱ, and within each of these iterations, we applied 30 CG iterations for the respective updates. The regularization parameters were tuned separately to balance the artifact and effective spatial resolution. Then we used UNFOLD to remove the undersampling artifact from the alternating sampling pattern.
Experiments: We compared our proposed joint reconstruction with separate reconstruction of each echo. The pulse sequences were programmed via TOPPE [7] and implemented on a GE UHP 3.0T scanner with a Nova 32RX head coil.

Results

Fig. 2 presents the reconstructed echo images from both separate and joint reconstructions. Echo 1 images resulting from joint reconstruction appear smoother and exhibit fewer streaking artifacts than those from separate reconstruction, likely due to using doubled data during the process. Echo 2 images from 2 methods both suffer from undersampling artifacts and also signal loss.
Fig. 3 displays the tSNR maps derived from the first echo images. Prior to the application of UNFOLD, these maps remain noisy, due to the alternating sampling pattern. As such, the merits of joint reconstruction are not immediately apparent. However, after UNFOLD, tSNR from the joint reconstruction clearly surpasses that of separate reconstruction, particularly near the brain's periphery. By using joint reconstruction, the mean tSNR of a centered elliptical ROI increased from 12.7 to 13.9 before UNFOLD, and 18.0 to 18.5 after UNFOLD.
Fig. 4 illustrates the T2* map estimation and its corresponding tSNR after UNFOLD. The joint estimation approach delivers a superior T2* tSNR within the brain relative to separate reconstruction. The mean tSNR of a centered elliptical ROI increased from 16.1 to 18.4.

Conclusion

The proposed approach demonstrates enhancements in the reconstructed echo images and the estimated T2* maps, evident both before and after applying UNFOLD. Future research may benefit from investigating additional regularization techniques to address the sub-problems more effectively. These could include edge-preserving regularizers and distinct regularizers for the real and imaginary components of the z map.

Acknowledgements

This work is supported in part by NIH Grant R01 EB023618.

References

[1] Peelle, J. E. (2014). Methodological challenges and solutions in auditory functional magnetic resonance imaging. Frontiers in neuroscience, 8, 253.

[2] Dionisio-Parra, B., Wiesinger, F., Sämann, P. G., Czisch, M., & Solana, A. B. (2020). Looping star fMRI in cognitive tasks and resting state. Journal ofMagnetic Resonance Imaging, 52(3), 739-751.

[3] Xiang, Haowei, Fessler, A., Jeffrey, Noll, C., Douglas. "Spatial-temporal reconstruction using UNFOLD in looping-star silent fMRI." ISMRM 2023

[4] Chan, R. W., Ramsay, E. A., Cunningham, C. H., & Plewes, D. B. (2009). Temporal stability of adaptive 3D radial MRI using multidimensional goldenmeans. Magnetic Resonance in Medicine, 61(2), 354-363.

[5] Madore, Bruno, Gary H. Glover, and Norbert J. Pelc. "Unaliasing by Fourier-encoding the overlaps using the temporal dimension (UNFOLD), applied to cardiac imaging and fMRI." Magnetic Resonance in Medicine, 42.5 (1999): 813-828.

[6] Xiang, Haowei, Fessler, A., Jeffrey, Noll, C., Douglas. "Model-based Image Reconstruction in Looping-star MRI." Magnetic Resonance in Medicine. DOI: 10.1002/mrm.29927

[7] Nielsen, J. F., & Noll, D. C. (2018). TOPPE: A framework for rapid prototyping of MR pulse sequences. Magnetic resonance in medicine, 79(6), 3128-3134.

Figures

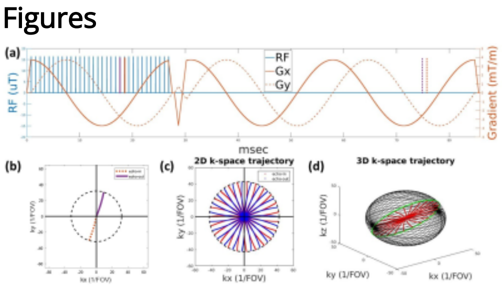

Figure 1: (a) A pulse sequence for a 2D plane of the 3D acquisition with one excitation/FID module and two GRE/data acquisition module (ramp-up &down gradient is required by TOPPE), the max slew rate for all modules (including ramps) is 5 mT/m/ms; (b) Illustration of overlapping echoes in GREmodule: the echo-out signal from purple RF pulse overlaps the echo-in signal from orange RF pulse in time; (c) 2D GRE k-space trajectory: odd number ofspokes are used to generate more evenly distributed spokes; (d) 3D k-space trajectory using 3D generalized golden-angle.

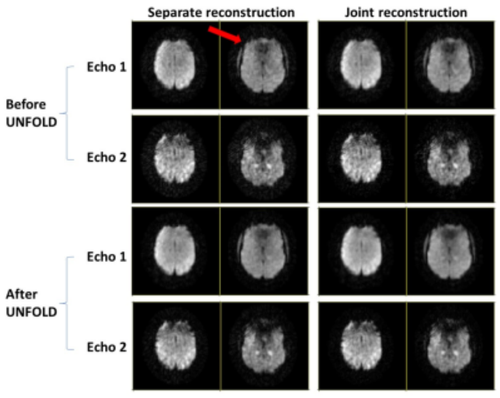

Figure 2 presents the reconstructed echo images from both separate and joint reconstructions. Before UNFOLD, echo 1 images resulting from joint reconstruction appear smoother and exhibit fewer streaking artifacts (red arrow) than those from separate reconstruction, likely due to the utilization of double the data during the process. Echo 2 images from 2 methods both suffer from undersampling artifact and also signal loss. After UNFOLD, the joint reconstruction shows reduced image noise and artifact relative to separate reconstruction.

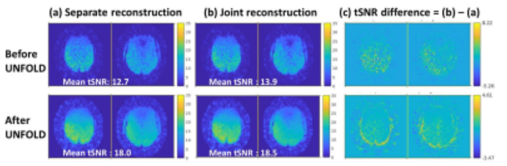

Figure 3 displays the tSNR maps derived from the first echo images. Prior to the application of UNFOLD, these maps remain noisy, attributable to undersampling artifacts from the alternating sampling pattern. As such, the merits of joint reconstruction are not immediately apparent. However, after UNFOLD, tSNR from the joint reconstruction clearly surpasses that of separate reconstruction, particularly near the brain's periphery. By using joint reconstruction, the mean tSNR of an centered elliptical ROI increased from 12.7 to 13.9 before UNFOLD, and 18.0 to 18.5 after UNFOLD.

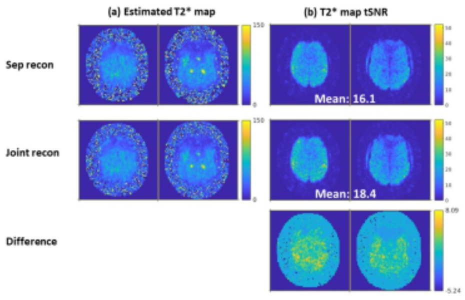

Figure 4 illustrates the T2* map estimation after UNFOLD and its corresponding tSNR. (a): The T2* map from joint reconstruction shows slightly more smooth T2* estimation. (b) The joint estimation approach delivers a superior T2* tSNR within the brain relative to separate reconstruction. The mean tSNR of a centered elliptical ROI increased from 16.1 to 18.4.

Proc. Intl. Soc. Mag. Reson. Med. 32 (2024)
0630